

Atomic Potential Wells and the Periodic Table*

A. R. P. RAU AND U. FANO

Department of Physics, The University of Chicago, Chicago, Illinois

(Received 19 July 1967; revised manuscript received 25 October 1967)

The trend of various atomic properties (e.g., electron potentials, binding energies, scattering phase shifts) along the periodic system is examined utilizing available evidence from experiments and computations. Properties that depend primarily on *different layers* of the atomic structure are seen to attain extreme values at *different columns* of the periodic table. From this plausible connection, one can see where and how to search for additional striking variations of properties from one element to the next; e.g., experiments on elastic scattering of slow electrons are thus indicated. The analysis also contributes to the interpretation and correlation of various atomic properties.

1. INTRODUCTION

THE periodic table has been constructed on the basis of chemical properties which reside in the outermost layers of atoms. The noble gases, which terminate the successive rows of the table, are also singled out in physics as the elements with peak ionization potential, another characteristic of atomic surfaces. The occurrence of noble gases upon completion of p , rather than of d or f , subshells (or indeed of full shells beyond $n=2$) derives from the circumstance that occupied d and f orbitals lie somewhat below the surface of atoms. For this reason the lanthanides and actinides are usually fitted into single boxes of the periodic table and transition elements are also often presented as insertions.

Elements that occur upon completion of d or f subshells may nevertheless be singled out by exhibiting peak values of properties that depend primarily on subsurface layers of their atoms. This paper identifies some of these properties on the basis of existing experimental and computational data. Indeed our attention was directed to a search for this systematic by chance observation that a certain property of calculated photoabsorption spectra has an extremum for Au.¹

2. SYSTEMATICS OF POTENTIAL WELLS

Since the calculations of Ref. 1 utilized the Herman-Skillman potential,² which is tabulated for all elements, the natural first step consists of examining variations of this potential along the periodic system. Thus we consider the mean potential energy $V(Z,r)$ of an electron as a function of its distance r from the nucleus within an atom of atomic number Z . (The definition of this quantity is not precise, as discussed below.) The tables of Ref. 2, from which Fig. 1 was constructed, result from Hartree-Fock-Slater calculations, which take into account the shell structure of atoms and represent exchange effects by an average term in the potential. This averaging constitutes an approximation, but some

such approximation is unavoidable if one wants to consider a local potential, since, e.g., a Hartree-Fock field is nonlocal. Averages are also performed in Ref. 2 over the potentials acting upon electrons of different shells and over the orientation of nonspherical fields. All these approximations imply that the features displayed in Fig. 1 or discussed below need not be significant in every detail. Presumably the major conclusions of this paper will stand independently of the underlying model, but anyhow we aim at drawing attention to the content of data in current use.

To begin with, notice in Fig. 1 that periodic variations of $V(Z,r)$ as a function of Z at constant r are far from negligible, ranging up to $\sim 20\%$. Peak potentials at given Z form ridges of the surface, which run in the r direction. Such ridges occur not only at the noble gases but even more outstandingly at the noble metals, i.e., upon completion of d subshells. As suggested by the remarks in Sec. 1, the ridges corresponding to noble metals begin and end at smaller radii than those for the noble gases. (On the whole, however, all features of the potential shift to larger radii r with increasing Z .) Completion of the $4f$ subshell at the end of the lanthanides ($Z\sim 70$) is marked only by a broad shoulder [at $r\sim 1$ atomic unit (a.u.)] rather than by a clear ridge; however, other evidence singling out this completion is presented in Sec. 4.

At large values of r the effective potential of an electron in any neutral atom becomes hydrogenic; the value of r at which this limit is attained for a particular atom may be regarded as its ionic radius. The horizontal segments of curves $V(Z,r)$ for large constant values of r in Fig. 1 correspond to sequences of elements for which this limiting behavior has been reached. These segments constitute increasingly large portions of the curves $V(Z,r=\text{const})$ for increasing values of r . They appear at lowest r through the flattening of ridges, first for the noble metals (which are known to have minimum ionic radii) and then for the noble gases.³

Besides the main ridges mentioned thus far, one notices in Fig. 1 smaller ridges corresponding to the half-filling of the $3d$, $4d$, and $4f$ subshells. These features

* This work was supported by the U. S. Atomic Energy Commission, Report No. COO-1674-3.

¹ S. T. Manson and J. W. Cooper, Phys. Rev. **165**, 126 (1968). We are very grateful to these authors for communication of their results prior to publication.

² F. Herman and S. Skillman, *Atomic Structure Calculations* (Prentice-Hall Inc., Englewood Cliffs, N. J., 1963).

³ However, the ionic radii given in standard tabulations are generally defined otherwise than through the characteristic of Herman-Skillman potentials considered here.

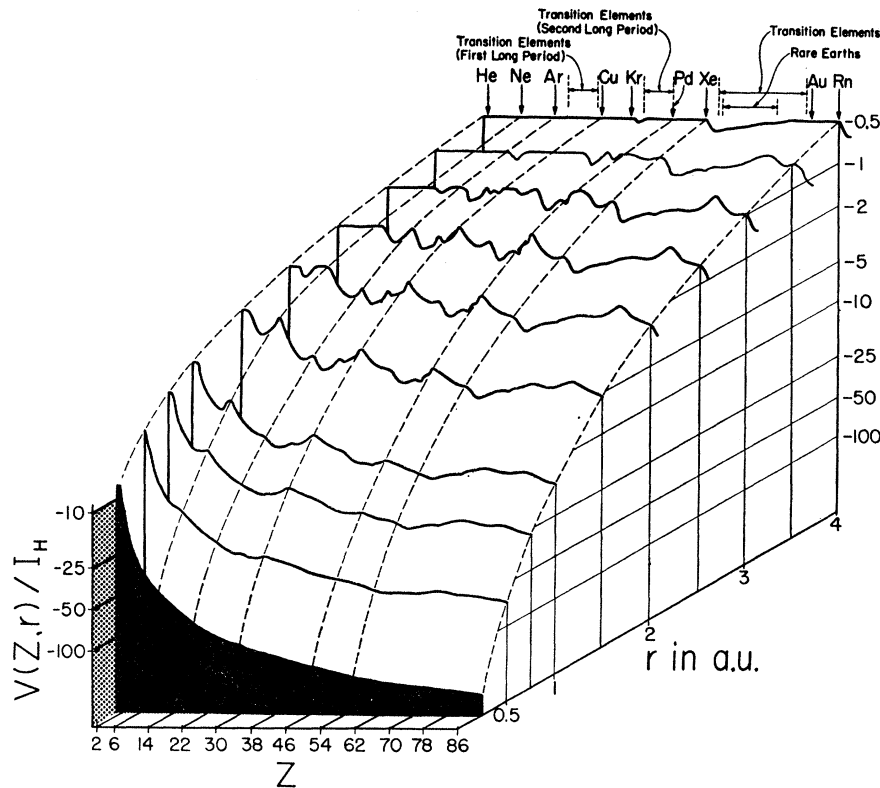


FIG. 1. Relief map of $V(Z, r)$
(1 a.u. $\approx 0.53 \text{ \AA}$).

as well as other localized irregularities correspond to known and understood local perturbations in the orderly filling of shells. One such local perturbation is observed at the end of the second transition group which occurs at Pd instead of Ag.

The behavior of $V(Z, r)$ can be analyzed in terms of its dependence on the distribution of electron density $\rho(r)$, which is given in Rydberg units by

$$V(Z, r) = -\frac{2Z}{r} + \frac{2}{r} \int_0^r \rho(r) 4\pi r^2 dr + 2 \int_r^\infty \rho(r) 4\pi r dr - 6[3\rho(r)/8\pi]^{1/3}. \quad (1)$$

As indicated above, the establishment and application of this formula involves somewhat arbitrary assumptions. Specifically, the self-Coulomb potential energy of the "probe" electron, which would be subtracted out automatically in a Hartree-Fock calculation, is corrected for only approximately by (1). This approximation is particularly poor for large r , since (1) vanishes exponentially at $r \rightarrow \infty$, whereas actually $V(Z, r) \rightarrow -2/r$. Reference 2 then corrects this larger error by applying (1) only for radii $r < r_0$ at which $|V(r)| > 2/r$, and setting $V(r) = -2/r$ for $r > r_0$.

The two integral terms in (1) represent inner and outer screening, respectively, and the last term represents the exchange potential which depends on the local

density in the Slater model. This exchange term varies by several hundredths of 1 Ry from one element to the next. The major variations observed in Fig. 1 are almost one order of magnitude larger than the exchange ones and derive from changes in screening. They may be related to the average number of electrons outside a sphere of radius r , $\int_r^\infty \rho(r) 4\pi r^2 dr$, which may even vary by one unit out of 2-4 from one element to the next at $r=2$. Table I shows sample data on this matter.

All these considerations and illustrative data pertain, as stated, to neutral atoms, i.e., to the field of a singly charged ion as seen by the remaining "test" electron. They would be altered to some extent, unknown at this time, for the potential wells of multiply charged ions. In fact, attention has been drawn, again recently,⁴ to the dependence of the order of orbital filling upon the net charge of the system. In the following we shall, however, disregard occasionally the difference between a neutral atom and a neutral atom plus an incident electron.

3. POTENTIAL WELL PLUS CENTRIFUGAL BARRIER

The effect of variations of $V(Z, r)$ as a function of Z is magnified when the influence of the attractive atomic field is combined with that of the repulsive centrifugal force. These two opposite forces often happen to balance

⁴ S. A. Goudsmit and P. I. Richards, Proc. Natl. Acad. Sci. U. S. 51, 664 (1964).

TABLE I. Sample data on the various contributions to the potential energy [as in (1)] at $r=2$ a.u. The values have been calculated from the tabulations in Ref. 2. All potential energies are in units of I_H ($I_H \approx 13.6$ eV).

Element	$-2Z/r$	Inner screening term	Outer screening term	Exchange	$V(Z,r)$	Average number of electrons "outside" $r=2$ a.u.
Se	-34	31.51	2.00	-1.33	-1.82	2.49
Kr	-36	33.74	1.83	-1.34	-1.77	2.26
Sr	-38	34.64	2.22	-1.14	-2.28	3.36
Pd	-46	44.12	1.46	-1.18	-1.60	1.88
In	-49	46.08	2.05	-1.12	-1.99	2.92
I	-53	49.35	2.64	-1.30	-2.31	3.65
Xe	-54	50.17	2.85	-1.35	-2.33	3.83
Ba	-56	51.57	2.88	-1.35	-2.90	4.43
Os	-76	72.52	2.49	-1.26	-2.25	3.48
Au	-79	76.04	2.27	-1.27	-1.96	2.96
Tl	-81	77.31	2.72	-1.23	-2.20	3.69

each other critically in subsurface layers of atoms. This balance is maintained over a considerable layer thickness because $V(Z,r)$ depends on r approximately as r^{-2} , i.e., much like the centrifugal potential, in the relevant range of r . Figure 2 illustrates the combined effect of attraction and repulsion by plots of

$$V(Z,r)/I_H + l(l+1)/r^2, \quad (2)$$

which is the effective potential in the radial Schrödinger equation for a single electron of azimuthal quantum number l .

As shown in Fig. 2, the balance between the two terms of Eq. (2) expresses itself in the occurrence of barriers which separate two "potential valleys," for various combinations of Z and l . The barriers occur in the range of $r \sim 1-2$ a.u., which corresponds to the term "subsurface layer." The barrier height is very sensitive to variations of $V(Z,r)$ just because it results from the near cancellation of two large terms. The existence of this balance between the two terms of (2), its influence on the rare-earth properties, and the occurrence of barriers for $l=3$ have long been known from studies with the Thomas-Fermi model.^{5,6} Note that the Thomas-Fermi potential depends smoothly and monotonically on Z because it does not take into account the shell structure of atoms. Here we emphasize that the height and the very existence of the barrier depend on Z nonmonotonically. In particular, maximum barrier heights occur for Cu, Ag (or Pd), and Au in accordance with the remarks of Sec. 2.

The existence of the barrier and its sensitive dependence on Z manifest themselves through the following noteworthy atomic properties:

(a) *Photoabsorption* by an inner electron of an atom is hindered unless it provides sufficient energy for the electron to clear the barrier. Therefore, the occurrence of a barrier depresses photoabsorption spectra near

their thresholds.⁷ It was the variability of this effect from atom to atom, observed in Ref. 1, that gave rise to this study. Since photoabsorption by an inner electron depends on the amplitude of its final-state wave function within the atom, it is also affected by the occurrence of shape resonances described below.

(b) Conversely, the penetration of an incident electron into the atomic field and consequently its *scattering* will be affected if this electron cannot clear the barrier. Also, shape resonances can occur in the scattering of electrons with energy a little higher than the barrier. The elastic scattering cross section $d\sigma(Z,E,\vartheta)/d\vartheta$ of low-energy electrons by atoms or ions has not been studied extensively as a simultaneous function of Z and of the other variables. However, an indication of resonant behavior can be seen in the steep rise of the $l=2$ phase shift η_2 for electron-Ar collision obtained from Ramsauer-Kollath data⁸; this rise occurs at the wave number $k = \frac{3}{4}$, i.e., a little above the barrier height in Fig. 2. On the basis of Fig. 2 the same rise should be absent for Sc ($Z=21$); a similar rapid transition should occur for η_3 from Xe to La. Reference 8 also shows a graph of η_2 as obtained from a Hartree field calculation; for small k , this curve disagrees with the experimental data and with the qualitative conclusion we have drawn from the Herman-Skillman potential. Notice finally in Ref. 8 that no resonance occurs for η_1 .

(c) Bound eigenstates of a two-valley potential are approximately eigenstates of one valley or the other, or of both in case of degeneracy, provided the barrier is sufficiently high. (They are exact eigenstates in the limit of an infinite barrier.) Now the potential is very nearly hydrogenic throughout the outer valley. Therefore the energy of bound excited states is given by the Rydberg formula with *near-integral quantum defect* in the presence of an effective barrier. For this reason quantum defects of spectral series are observed to vary

⁵ E. Fermi, in *Quantentheorie und Chemie, Leipziger Vortraege*, edited by H. Falkenhagen (S. Hirzel Verlag, Leipzig, 1928), p. 95; also in *Collected Papers of Enrico Fermi* (The University of Chicago Press, Chicago, 1962), p. 291.

⁶ M. Goepfert-Mayer, Phys. Rev. **60**, 184 (1941).

⁷ Photoabsorption spectra are considered in detail in a comprehensive paper by U. Fano and J. W. Cooper (to be published).

⁸ N. F. Mott and H. S. W. Massey, *The Theory of Atomic Collisions* (Oxford University Press, London, 1965), 3rd ed., Fig. 94.

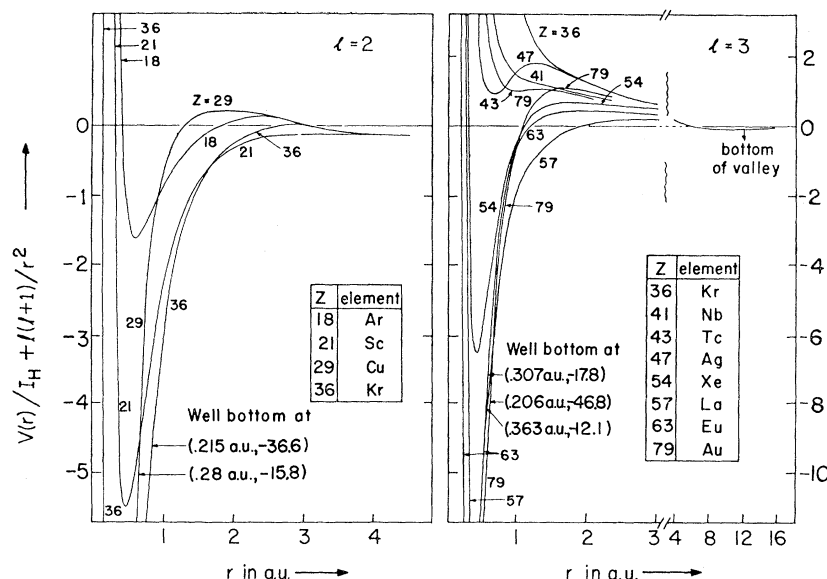


FIG. 2. Sum of electrostatic and centrifugal potentials for electrons with orbital quantum number l (1 a.u. $\approx 0.53 \text{ \AA}$).

by steps as functions of Z for values $l \geq 2$.⁹ The jump of quantum defects for $l=2$ and 3, and indeed the onset of transition and rare-earth groups after the alkaline earths, appear to be catalyzed by the increase of atomic radii after the noble gases and by the resulting drop of potential barriers.

4. EVIDENCE FROM X-RAY LEVELS

The binding energy of inner-shell electrons represents the work to be performed in removing such electrons to

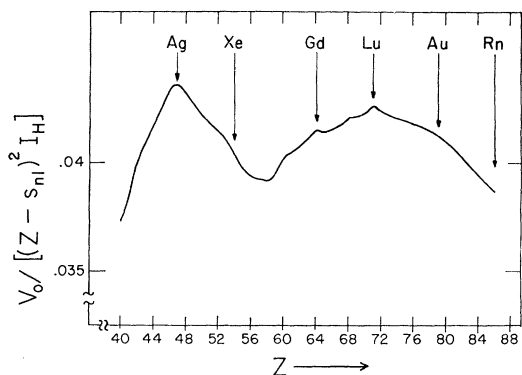


FIG. 3. Outer screening energy of $4s$ electrons.

⁹ We are indebted to W. C. Martin for drawing our attention to this fact and particularly to its occurrence for $l=2$, an observation that stimulated this study.

infinity. It thereby depends on the field in more external layers of the atom through an outer screening effect. According to a familiar schematization,¹⁰ one represents the binding energy in absence of outer screening by a hydrogenic ("Moseley law") formula $-(Z-s_{nl})^2 I_H/n^2$, where s_{nl} is a suitable inner screening correction¹¹ and $I_H = 13.6 \text{ eV}$. Any difference V_0 between this formula, which depends on Z monotonically and smoothly, and the experimental value is thereby attributed to outer screening. That is, one expresses the experimental values of the energy levels by

$$E_{nl} = -(Z-s_{nl})^2 I_H/n^2 + V_0. \quad (3)$$

Figure 3, akin to a previous tabulation,¹² shows a plot of V_0 versus Z for the N_I levels¹³ ($n=4$, $l=0$), in the Kr to Rn rows of the periodic table. Notice that here the second peak occurs at Lu ($Z=71$), upon completion of the $4f$ subshell, rather than at Au where $5d$ is completed. Thus completion of the $4f$ subshell has a major effect on the $4s$ electrons whose average radial distance in the relevant atoms is $\sim \frac{1}{4} \text{ \AA}$ ($\approx 0.5 \text{ a.u.}$).

¹⁰ H. A. Bethe and E. E. Salpeter, *Quantum Mechanics of One- and Two-Electron Atoms* (Springer-Verlag, Berlin, 1957), Sec. 17 β .

¹¹ J. C. Slater, *Phys. Rev.* **36**, 57 (1930).

¹² Margaret N. Lewis, National Bureau of Standards, Report No. 2457, 1953, p. 72 (unpublished).

¹³ The E_{N_I} values for Fig. 3 are from T. A. Bearden and A. F. Burr, *Rev. Mod. Phys.* **39**, 125 (1967).